Published by :
http://www.ijert.org

International Journal of Engineering Research & Technology (IJERT)
ISSN: 2278-0181
Vol. 12 Issue 06, June-2023

Multibody Dynamic Simulation of A Mountain Bike To Reduce Riding Injuries During A Jump Event

Akshay Kargaonkar[1] , Nirmal Kumar Singh[1]

[1]Department of Mechanical Engineering, Indian Institute of Technology (ISM), Dhanbad

ABSTRACT

Mountain biking is becoming an extreme sport in the present time. As mountain biking is becoming increasingly popular, it's also becoming dangerous, as riders push themselves beyond their comfort, also increasing risks of injury. The paper presents a comparison of a bike jump's impact on rider's joints for different cases of landing on a solid surface. The paper shows a multibody dynamic model of a mountain bike and rider satisfying 95th percentile male dimensions, along with front and rear suspensions. The model incorporated all sources of stiffness and damping in suspensions and rider's joints. The model was created in ADAMS (Automatic Dynamic Analysis of Mechanical Systems), and then simulated for a bike jump at different landing angles to compare forces and torques on different bone joints of rider. Finally, an optimum case of landing was found with minimum possibility of fatality.

Keywords: Multibody Dynamics, Adams, mountain bike, simulation

1. INTRODUCTION

Mountain biking is an inherently dangerous sport with the distinct possibility of severe injuries or even worse. A study from Whistler Mountain Bike Park reported 2000 injuries to 900 riders in a singed 5-month season[8]. The injuries ranged from broken bones, concussion, internal bleeding and in some severe cases quadriplegia. Most of the injuries occur during landing after a jump. The mostly affect areas include knee joints, ankle joints and elbow joints. These injuries can be minimized by a great factor just by knowing the physics behind landing the bike properly after every jump. The paper presents a comparative study and simulation of different cases of landing a bike on a solid surface after a 4.6 meters jump. The torques and forces acting on different joints of rider are analyzed and compared to find the optimum case of safe landing.

2. METHODOLOGY

The paper presents a multibody dynamic model of a typical mountain bike along with a rider, modelled in solidworks and then exported to MSC ADAMS as a parasolid file for simulation. MSC ADAMS program is a widely used Multibody Dynamics (MBD) software where the user not only can assemble a physical description of the problem but can also write or change equations of constraints or motions. Here, the equations are generated in numerical format and are solved directly using numerical integration routine embedded in the package.

After exporting the model in ADAMS, different parameters were defined for the model including constraints on the movement of the system in the form of joints and contacts. Density and forces acting on different bodies in the model were defined further. ADAMS/Solver is used to solve the complex computations and equations of motion for dynamic analysis. Several different integrators are available for finding the solution to the full system of differential and algebraic equations (DAE's) [3].

International Journal of Engineering Research & Technology (IJERT)
ISSN: 2278-0181
Vol. 12 Issue 06, June-2023

An analysis, performed over time, of a system that relies on inertial effects to determine motion is called as dynamic analysis. Makkonen [2] added that the dynamic analysis provides the time-history solution for all of the displacements, velocities, accelerations, and internal reaction forces in a mechanical system driven by a set of external forces and excitations. After simulation, the results were extracted using ADAMS postprocessor and then further analyzed to get to a conclusion.

3. GOVERNING EQUATIONS

3.1. Constraint Equations

Joints and contacts restrict the relative motion between the bodies. From a mathematical perspective[1], such constraints are in form of algebraic equation as a function of position vector q.

$$\boldsymbol{\Phi \equiv \Phi(q) = 0} \tag{1}$$

Which is a matrix containing collection of all algebraic constraints. The number of equations are equal to the number of constraints induced by the joints. The first time derivative of (1) yields the velocity constraint equation expressed as[1]:

$$\boldsymbol{\Phi_q \dot{q} = 0} \tag{2}$$

Where $\boldsymbol{\Phi_q}$ denotes the Jacobian matrix $[\boldsymbol{\partial \Phi / \partial q}]$ and $\dot{\mathbf{q}}$ contains the velocity terms. The second time derivative of (1) results in [1]:

$$\boldsymbol{\Phi_q \ddot{q} + (\Phi_q \dot{q})_q \dot{q} = 0} \tag{3}$$

Or,

$$\boldsymbol{\Phi_q \ddot{q} = -(\Phi_q \dot{q})_q \dot{q}} \tag{4}$$

Nikravesh [1] referred the term $\boldsymbol{-(\Phi_q \dot{q})_q \dot{q}}$ as right side of kinematic acceleration equation, referred as:

$$\boldsymbol{\gamma = -(\Phi_q \dot{q})_q \dot{q}} \tag{5}$$

Therefore, form (4) and (5),

$$\boldsymbol{\Phi_q \ddot{q} = \gamma} \tag{6}$$

3.2. Equations of Motion

Newton Euler equations describe the combined translational and rotational dynamics of a rigid body[4]. These equations are the base for complicated 'multi-body' formulation that describe the system of rigid bodies connected by joints or other constraints.

Newton Euler equations are expressed in the general form as follows:

$$\boldsymbol{M\ddot{q} = g + g^{(c)}} \tag{7}$$

Where, M is the diagonal body mass matrix, q¨ denotes acceleration matrix, g denotes body force vector containing all the external forces acting on the system, and $\mathbf{g^{(c)}}$ denotes reaction forces or internal forces acting on a specific body as these equations are written in a specific body's frame of reference. The term $\mathbf{g^{(c)}}$ can be expressed in terms of Jacobian matrix and Lagrange multiplier as follows[1]:

$$\boldsymbol{g^{(c)} = \Phi_q{}^T \lambda} \tag{8}$$

Hence, the Newton Euler equations from (7) and (8) can be expressed as follows:–

International Journal of Engineering Research & Technology (IJERT)
ISSN: 2278-0181
Vol. 12 Issue 06, June-2023

$$\mathbf{M\ddot{q}} = \mathbf{g} + \mathbf{\Phi_q}^{\mathbf{T}}\boldsymbol{\lambda} \quad (9)$$

The above equations has been solved by ADAMS/Solver using the algorithm given in figure 1.

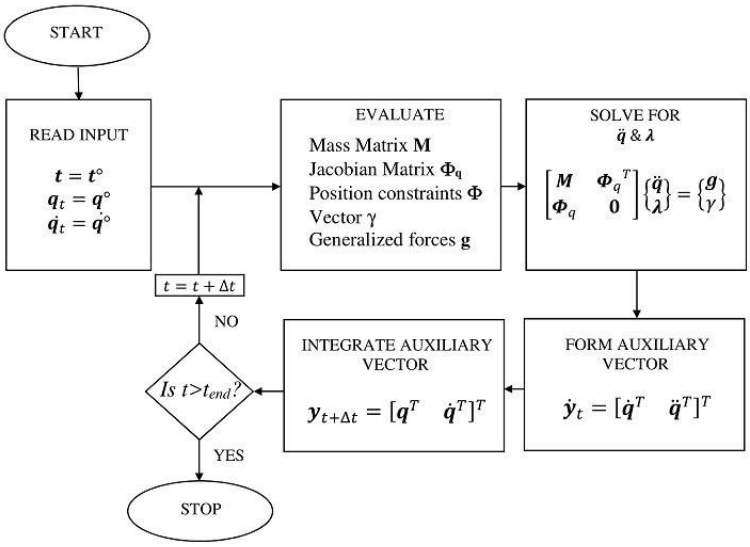

Fig. 1. Flowchart of computational procedure for dynamic analysis of a multibody system.

The constraint equations are non-linear in terms of **q**, hence are usually solved by Newton- Raphson method whereas other equations are linear in terms of $\dot{\mathbf{q}}$ and $\ddot{\mathbf{q}}$ are solved by any usual method.

4. MODELLING PROCESS

4.1. Computer Aided Design

Different parts of mountain bike and manikin were modelled and assembled in solidworks and later were imported to MSC ADAMS as a parasolid file. The x-axis represents pitch movement, y-axis represents yaw movement and z-axis represents roll movement. Mass properties were defined for manikin as well as for the mountain bike. Manikin, also called as rider model consists of nine rigid bodies on which constraints were imposed in the form of revolute joints. Manikin was attached with bike using revolute joints at bike handle and bike paddles. To simulate the model as close to real life situation, the manikin joints were given a stiffness and a damping value. The value of stiffness and damping coefficient were defined close to the values given in [6,9]. The inertial properties of rider were decided based on density. A density of 1000 kg/m3 (1 gm/ml) was taken based on the study[7].

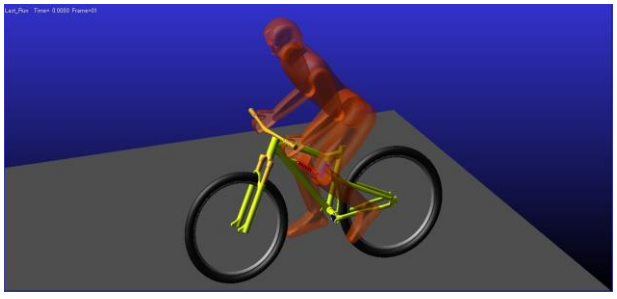

Fig. 2. CAD model of mountain bike with rider after importing in MSC ADAMS.

The inertial properties of the rider are given in table 1.

International Journal of Engineering Research & Technology (IJERT)
ISSN: 2278-0181
Vol. 12 Issue 06, June-2023

Table 1: Inertial properties of rider model

Component	Mass (Kg)	I_{xx}(Kg-mm^2)	I_{yy}(Kg-mm^2)	I_{zz}(Kg-mm^2)
Torso	47.21	2.33e + 06	2.08e + 06	6.22e + 05
Upper arm	3.60	4.37e + 04	4.02e + 04	6.62e + 03
Lower arm	2.20	3.29e + 04	3.17e + 04	2.42e + 03
Upper leg	16.12	4.54e + 05	4.47e + 05	7.73e + 04
Lower leg	7.45	1.89e + 05	1.75e + 05	3.06e + 04

Whereas, the stiffness and damping properties of the rider are given in table 2 [6,9]:

Table 2: Stiffness and Damping properties of rider model

Component	Stiffness coefficient (N-mm/deg)	Damping coefficient (N-mm-s/deg)
Arms	3.8e + 04	300
Legs	3.8e + 04	300
Hips	3.8e + 04	600

Different parts of bike and their inertial properties are given in table 3:

Table 3: Inertial properties of bike model

Component	Mass (Kg)	I_{xx}(Kg-mm^2)	I_{yy}(Kg-mm^2)	I_{zz}(Kg-mm^2)
Main frame	1.39	7.71e + 04	6.42e + 04	1.38e + 04
Rear frame	2.77	7.35e + 04	6.10e + 04	2.42e + 04
Rocker	0.29	3.43e + 02	3.36e + 02	1.17e + 02
Rear rocker	0.11	9.77e + 01	8.52e + 01	2.68e + 01
Handlebar	1.20	6.64e + 04	6.60e + 04	5.23e + 02
Headset	1.89	2.32e + 04	1.63e + 04	7.26e + 03
Suspension fork	4.95	7.91e + 04	5.96e + 04	2.13e + 04
Rim	0.55	5.21e + 04	2.64e + 04	2.64e + 04
Tire	0.78	9.41e + 04	4.78e + 04	4.78e + 04

International Journal of Engineering Research & Technology (IJERT)
ISSN: 2278-0181
Vol. 12 Issue 06, June-2023

4.2. Track Model

Track was modelled for a drop of 4.6 meters. Contacts were defined between track and tires with a stiffness coefficient of 100 N/mm and a damping coefficient of 1000 Ns/mm. The model was needed to be stable without losing contact with the track. Hence, friction forces were defined with high static coefficient of 1.0 and dynamic coefficient equal to 0.7.

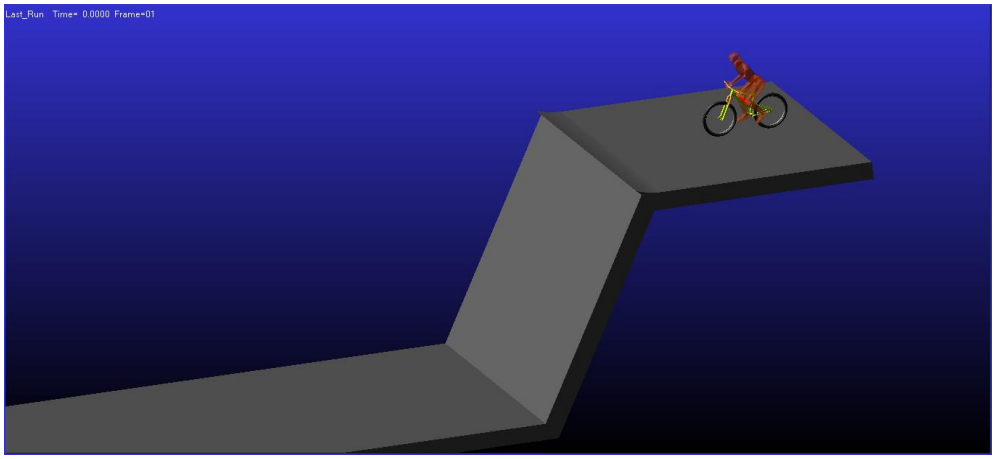

Fig. 3. CAD model of mountain bike, rider along with track after importing in MSC ADAMS.

4.3. Mountain bike suspension

A typical mountain bike have forward suspension as well as rear suspension. Rear suspension is commonly referred to as the rear shock. The shock allows the rear wheel to soak up impacts, helping to keep the tire in contact with the ground, increasing rider control and decreasing rider fatigue. The rear frame triangle, which holds the rear tire, pivots around one point to enable rear wheel to travel through a range of motion. The rear frame triangle is connected to a rocker, which transfers motion to the spring damper system connected to the main frame, and rocker. The front suspension system is rather simple and is connected between suspension fork and headset. The stiffness and damping values were decided based on the wheel travel and static stability of the model when released on the track from a small height of 40 mm. Figure 4 and Figure 5 shows fluctuation of normal reaction force on front tire due to different values of damping coefficient. Finally, the values shown in Table 4 were chosen based on the above-mentioned factors.

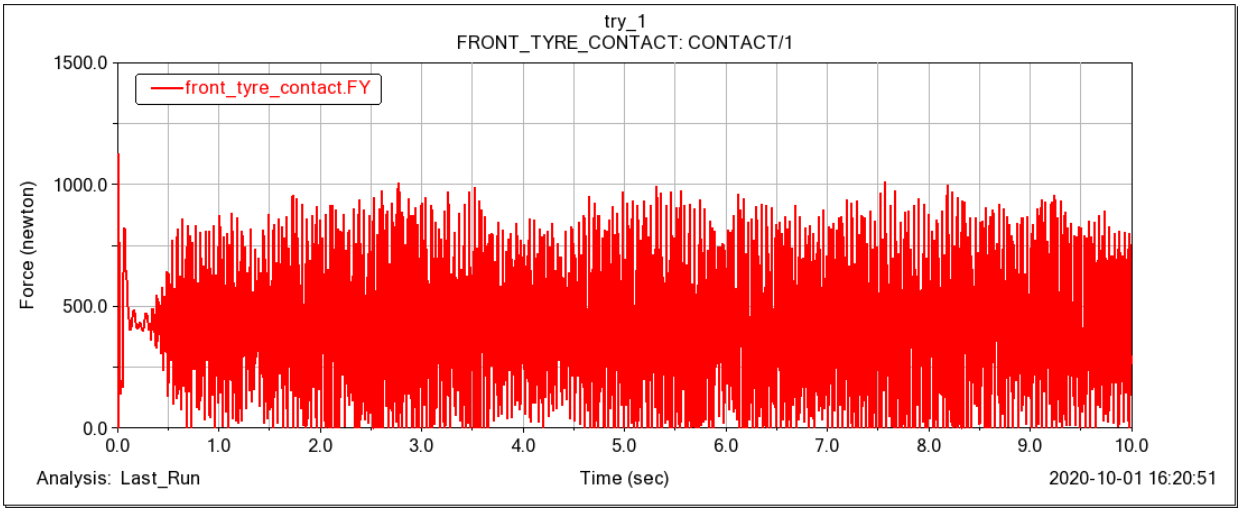

International Journal of Engineering Research & Technology (IJERT)
ISSN: 2278-0181
Vol. 12 Issue 06, June-2023

Fig. 4. Graph of normal force on front tire for a damping coefficient of 50 Ns/mm.

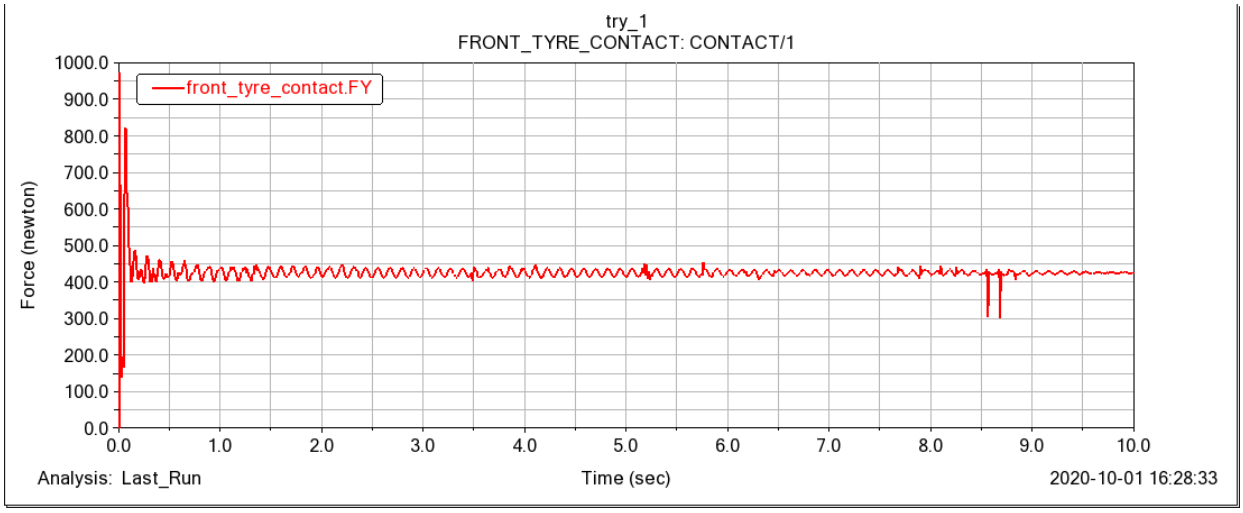

Fig. 5. Graph of normal force on front tire for a damping coefficient of 100 Ns/mm.

Table 4 shows stiffness and damping values for suspension system.

Table 4: Stiffness and damping properties of suspension system.

Component	Stiffness coefficient (N/mm)	Damping coefficient (Ns/mm)
Front shock	50	100
Rear shock	100	100

Fig. 6. Position of front and rear spring-damper system in mountain bike.

International Journal of Engineering Research & Technology (IJERT)
ISSN: 2278-0181
Vol. 12 Issue 06, June-2023

4.4. Balanced Model

The model was not symmetric about the y-z plane. Hence, performed roll movement after some time. Therefore, to keep the model balanced every time, a torque was applied in z direction as a function of roll angle. This torque countered the unbalanced inertia and kept the model standing without affecting the other values. Figure 7 shows change in torque's value to balance the model.

Fig. 7. Graph of balancing torque with respect to time when bike is released on track.

The rear wheel was given an angular acceleration of 110 deg/s2, which is equal to an acceleration of 0.7 m/s2. Results were obtained for a duration of 2.4 seconds where for each case, tire touched the track at approximately 2.2 seconds. In order to simulate different cases of landing at different pitch angle, a torque about x-axis was applied on the frame to change the pitch angle of bike during landing. The results were obtained for four different cases. The first case represents landing on the front tire with a pitch angle of negative 25 degrees. The second case represents landing at approximately 0 degrees of pitch angle where both the tires touches ground simultaneously. The third case represents landing on the rear tire followed by front tire with an approximate pitch angle of 10 degrees. The fourth case represents landing on only rear tire where most of the impact is absorbed by the rear damper followed slamming of front tire on track at a very high speed.

5. RESULTS

Figure 8 shows changes in pitch angle for all the four cases. Figure 9 shows variation in front suspension forces of the bike. Figure 10 shows variation in rear suspension forces of the bike. Figure 11, Figure 12 and Figure 13 represents torque values on elbow joint, hip joint and knee joint of the manikin model respectively. Sudden changes in values were seen at approximately 2.2 seconds, when the bike touched the track.

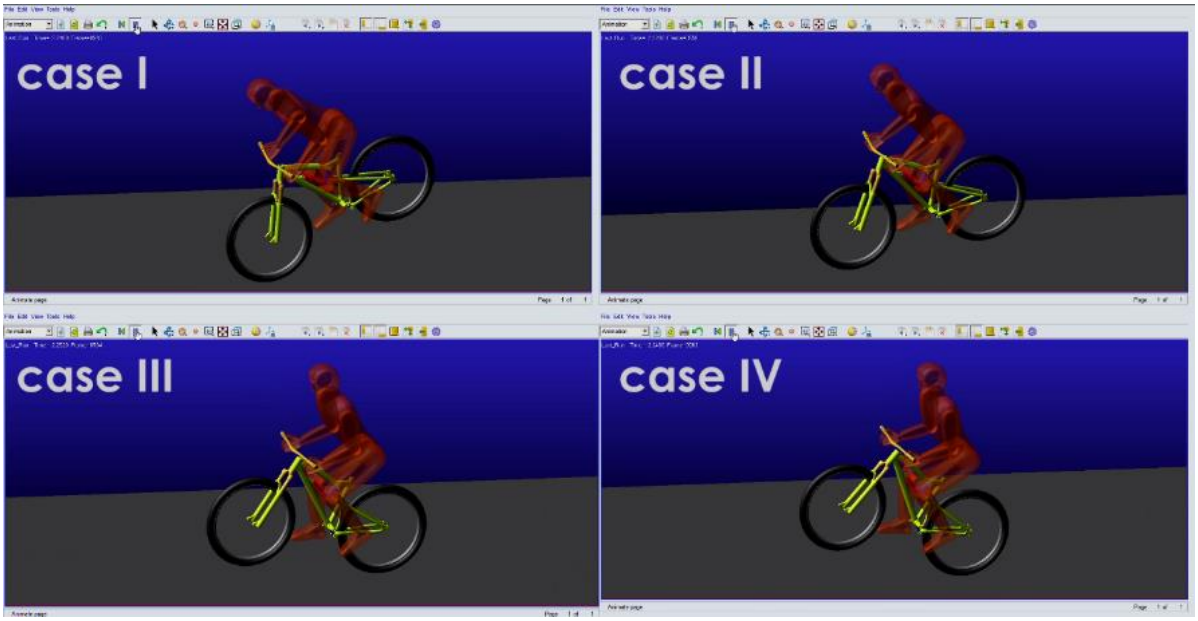

Fig. 8. Different landing cases of the mountain bike for different pitch angles.

International Journal of Engineering Research & Technology (IJERT)
ISSN: 2278-0181
Vol. 12 Issue 06, June-2023

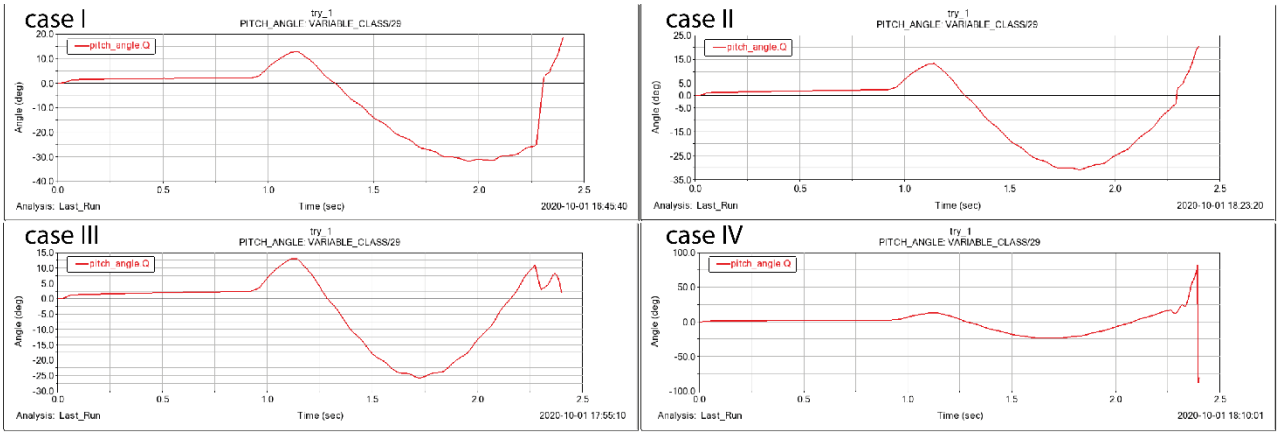

Fig. 9. Variation of pitch angle with respect to time for different cases of landing.

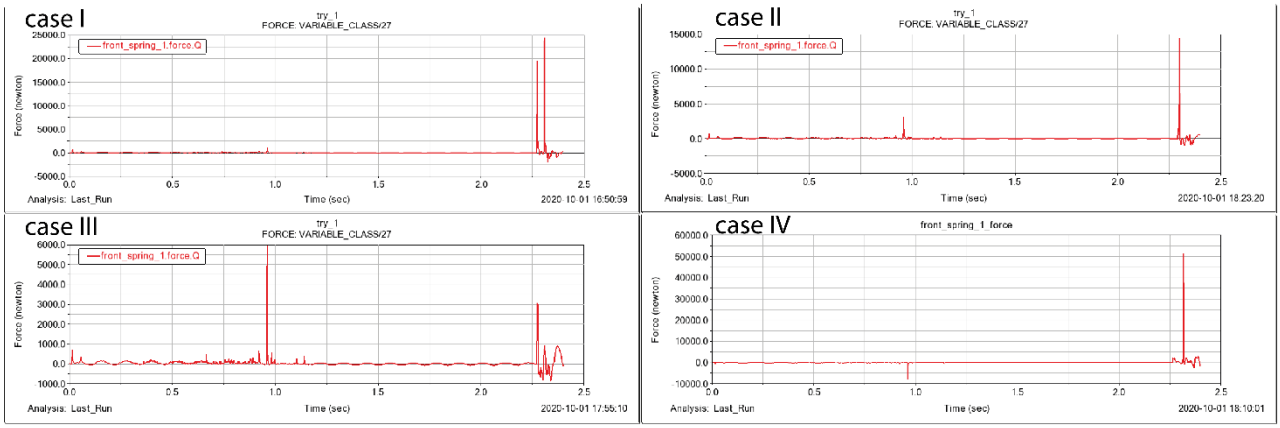

Fig. 10. Variation of front spring-damper system forces with respect to time for different cases of landing.

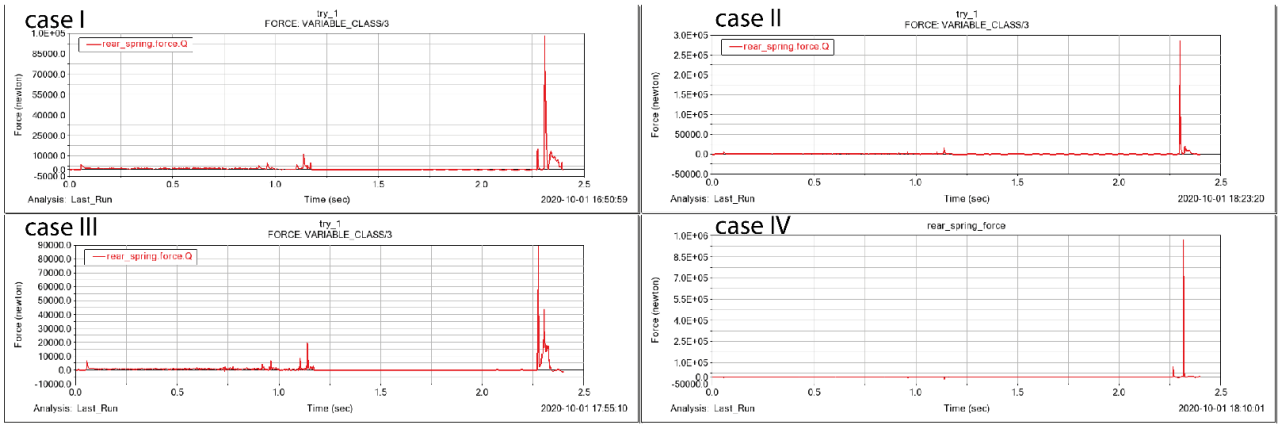

Fig. 11. Variation of rear spring-damper system forces with respect to time for different cases of landing.

International Journal of Engineering Research & Technology (IJERT)
ISSN: 2278-0181
Vol. 12 Issue 06, June-2023

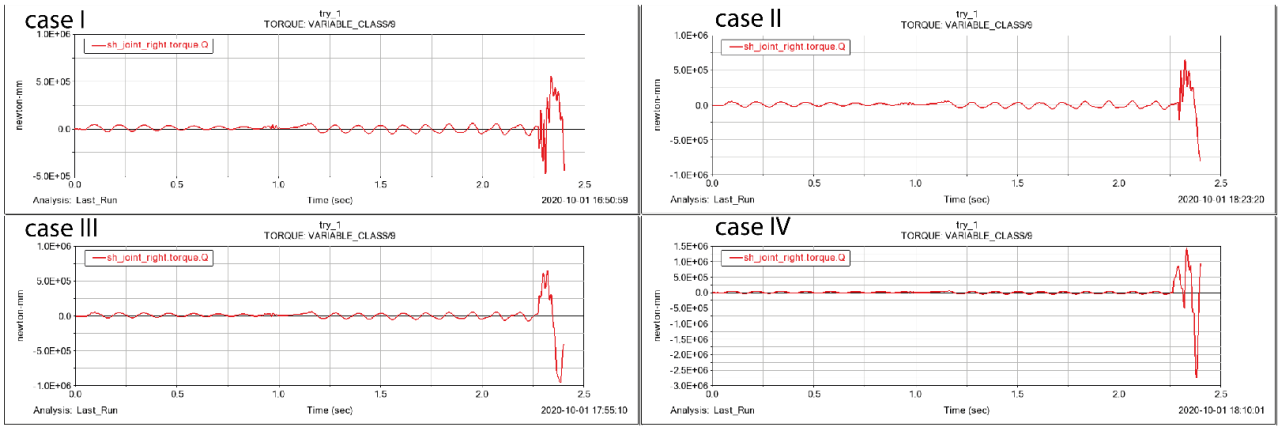

Fig. 12. Variation of torque on elbow joint with respect to time for different cases of landing.

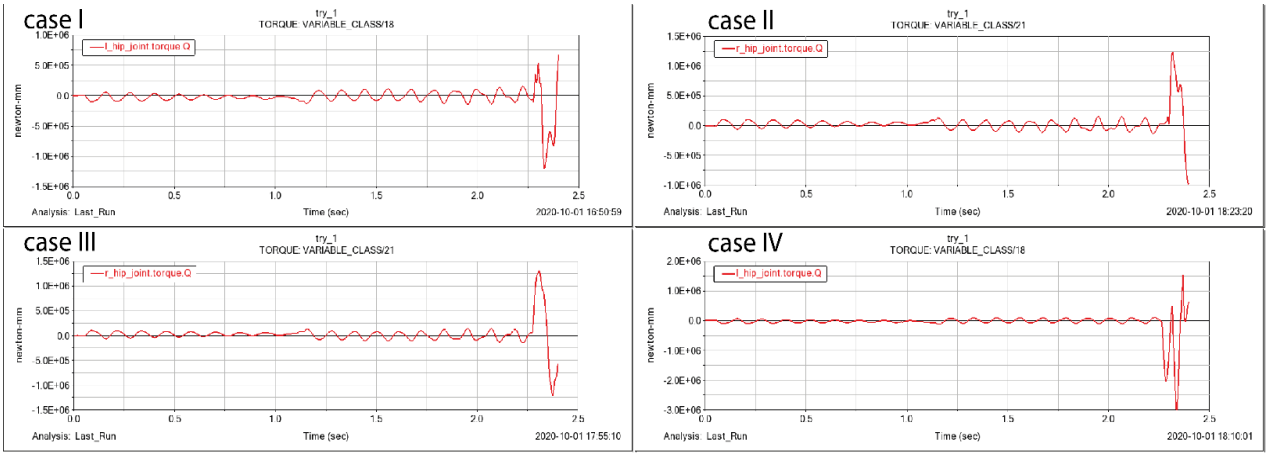

Fig. 13. Variation of torque on hip joint with respect to time for different cases of landing.

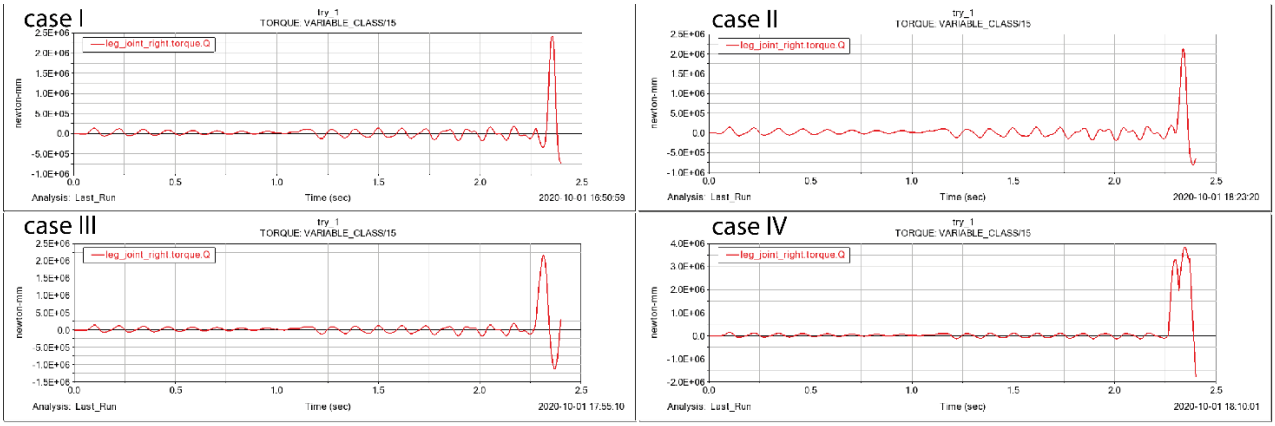

Fig. 14. Variation of torque on knee joint with respect to time for different cases of landing.

International Journal of Engineering Research & Technology (IJERT)
ISSN: 2278-0181
Vol. 12 Issue 06, June-2023

Table 5 summarizes the above results obtained for different cases of landing a mountain bike on solid track.

Table 5: Different results obtained for the four cases.

Parameters	**Case I**	**Case II**	**Case III**	**Case IV**
Pitch angle (degrees)	-25	0	10	23
Front shock force (N)	2.5e+04	1.5e+04	3.0e+03	5.0e+04
Rear shock force (N)	1.0e+05	3.0e+05	9.0e+04	1.0e+06
Elbow joint torque (N-mm)	5.1e+05	5.3e+05	5.2e+05	5.0e+06
Hip joint torque (N-mm)	1.3e+06	1.3e+06	1.3e+06	3.0e+06
Knee joint torque (N-mm)	2.5e+06	2.2e+06	2.2e+06	4.0e+06

6. CONCLUSION

The results of the study provide valuable insights into the impact of bike jumps on the rider, specifically considering different pitch angles. Among the investigated cases, the third case, characterized by a positive 10-degree pitch angle, exhibits the least impact on the rider. In terms of joint torque, the results show that the torque exerted on the hip joint remains relatively consistent across the first, second, and third cases, amounting to approximately half the value observed in the fourth case. Similarly, the torque on the knee joint is minimized in the second and third cases, reaching roughly half of the maximum value recorded in the fourth case. While the first case shows the least torque on the elbow joint, the third case stands out in other aspects. It demonstrates dominance in other fields, indicating superior performance compared to the other cases. Moreover, a notable disparity can be observed in suspension forces. The force resulting from the impact is well balanced in the third case, suggesting an optimized suspension system design for mitigating the effects of the jump.

These findings underscore the importance of considering pitch angles and their influence on rider impact, joint torques, and suspension forces. The third case, with a positive 10-degree pitch angle, emerges as the most favorable configuration, showcasing reduced impact on the rider and optimized performance in various aspects.

7. DISCUSSION

The paper presents a multibody dynamic model of a mountain bike with a rider, aiming to simulate different landing scenarios. While the model does not precisely replicate real-world conditions, the results obtained from comparing various landing cases closely align with reality. By utilizing the mountain bike model implemented in ADAMS, the study highlights the impact of the jump event on the rider's joints, focusing on the elbow, hip, and knee joints.

The findings clearly indicate that the third case, characterized by a pitch angle of approximately 10 degrees, represents the optimal landing scenario for a mountain bike on a solid surface. This particular configuration exhibits favorable outcomes in terms of joint stress and impact on the rider.

International Journal of Engineering Research & Technology (IJERT)
ISSN: 2278-0181
Vol. 12 Issue 06, June-2023

Looking ahead, such simulations hold promise not only for assisting in the design process of mountain bikes but also for enhancing rider safety. By gaining insights into how different landing scenarios affect the rider's joints, manufacturers can refine their designs to minimize potential risks and enhance the overall riding experience.

REFERENCES

[1] Parviz E. Nikravesh, “Computer-aided analysis of mechanical systems,” Prentice-Hall, Inc., USA, 1988.
[2] Makkonen P, “Integrated CAD methodology for simulation driven product development,” OST-95 Conference on Machine Design, Oulu, Finland, 1995.
[3] Department of Mechanical Engineering, University of Rochester, http://www2.me.rochester.edu/courses/ME204/nx_help/en_US/graphics/fileLibrary/nx/tdoc_motion/mss.pdf, October 6, 2020
[4] Shabana AA, “Dynamics of multibody systems,” Wiley, New York, 1989.
[5] Paulo Flores, “Concepts and Formulations for Spatial Multibody Dynamics,” Springer International Publishing, 2015.
[6] Wang EL, Hull ML, “A dynamic system model of an off-road cyclist,” J Biomech Eng 119(3):248−25, 1997.
[7] H. J. Krzywicki, K. S. K. Chinn, “Human Body Density and Fat of an Adult Male Population as Measured by Water Displacement,” 1967.
[8] Gaulrapp H, Weber A, Rosemeyer B., "Injuries in mountain biking." Knee surgery, sports traumatology, arthroscopy: official journal of the ESSKA, 2001.
[9] Corves B., Breuer J., Schoeler F., Ingenlath P., “A Three-Dimensional Multibody Model of a Full Suspension Mountain Bike,” In: Ceccarelli M., Hernández Martinez E. (eds) Multibody Mechatronic Systems. Mechanisms and Machine Science, vol 25. Springer, Cham, 2015